

Synthesis and properties of $\text{RbRP}_4\text{O}_{12}$ crystals

K. BYRAPPA*, B. N. LITVIN

*Department of Crystallography and Crystal Chemistry, Faculty of Geology,
Moscow State University, Moscow, USSR 117234*

We have investigated the system $\text{Rb}_2\text{O}-\text{R}_2\text{O}_3-\text{P}_2\text{O}_5-\text{H}_2\text{O}$ within the temperature range 300 to 800° C. A composition diagram showing fields of crystallization of different phases is given. The crystal chemistry of these crystals are discussed briefly. The crystals were characterized by various methods: IR spectroscopy, differential thermal analysis, laser spectroscopy and others. $\text{RbNdP}_4\text{O}_{12}$ crystals have a greater number of polymorphic modifications than any other tetraphosphates.

1. Introduction

In recent years mixed alkaline rare earth phosphates — $\text{MRP}_4\text{O}_{12}$ (where M = Li, Na, K, Rb, Cs and Tl; R = rare earth ion) have attracted much attention due to the possibilities of using them as miniature laser materials, colour luminophors, fibre optic communication materials etc. Many mixed alkaline rare earth phosphates are reported in the literature, but a systematic study of these phosphates with reference to phase formation in a four-component system, growth of monocrystals and properties has not been carried out for all the representatives. Such data are available only for $\text{CsRP}_4\text{O}_{12}$, $\text{LiNdP}_4\text{O}_{12}$ and $\text{KNdP}_4\text{O}_{12}$ crystals [1-5]. The present work deals with the study of phase formation in the system $\text{Rb}_2\text{O}-\text{R}_2\text{O}_3-\text{P}_2\text{O}_5-\text{H}_2\text{O}$ (within the temperature range 300 to 800° C), and the synthesis and properties of $\text{RbRP}_4\text{O}_{12}$ crystals.

2. Experimental methods

The phase formation in the system $\text{Rb}_2\text{O}-\text{R}_2\text{O}_3-\text{P}_2\text{O}_5-\text{H}_2\text{O}$ within the temperature range 300 to 800° C and at ~1 atm pressure was studied according to our earlier methods [6, 7]. To study this system in detail we selected neodymium as a representative rare earth ion. The system $\text{Rb}_2\text{O}-\text{Nd}_2\text{O}_3-\text{P}_2\text{O}_5-\text{H}_2\text{O}$ corresponds to a four-component system with H_2O and P_2O_5 as the evaporating components. According to Gibb's phase rule, with temperature and pressure as constants only four phases can exist in equilibrium,

out of which one must be a liquid phase and the other three crystalline phases. The necessary amount of starting materials such as orthophosphoric acid (85% concentration) and rubidium carbonate were placed in a vitreous carbon glass crucible and the solution was held at room temperature until the CO_2 evaporated. Later Nd_2O_3 was added to this solution. The crucible was heated at a predetermined temperature in the furnace for 8 to 10 days. After the run the resultant products were cleaned and analysed. The results of the experiments are represented in Fig. 1, an AB diagram (where A = $\text{Rb}_2\text{O}/\text{Nd}_2\text{O}_3$ and B = $\text{P}_2\text{O}_5/\text{Rb}_2\text{O} + \text{Nd}_2\text{O}_3$) showing fields of crystallization of different crystalline phases. The variations in the concentration of P_2O_5 and Rb_2O determine the boundaries of crystallization of different phases. A more detailed study of the phase formation shows that in the field of crystallization of mixed polyphosphates, four polymorphic modifications of $\text{RbNdP}_4\text{O}_{12}$: $\text{RbNd}[\text{P}_4\text{O}_{12}]$ -C; $\text{RbNd}[\text{P}_4\text{O}_{12}]$ -A; $\text{RbNd}(\text{PO}_3)_4$ -IV and $\text{RbNd}(\text{PO}_3)_4$ -VI[†] crystallize simultaneously under the same physico-chemical conditions. The number of polymorphic modifications of $\text{RbNdP}_4\text{O}_{12}$ in this system is higher than for any other tetraphosphates $\text{MNdP}_4\text{O}_{12}$ (where M = Na, Li, K, Cs and Tl). The X-ray data for all the four modifications of $\text{RbNdP}_4\text{O}_{12}$ are given in Table I. Unfortunately, determination of the monophase crystallization field was not possible. This is mainly due to the similarity in many of the structural characteristics. The neodymium

*Present address: The Mineralogical Institute, University of Mysore, Manasa Gangotri, Mysore, India, 570006.

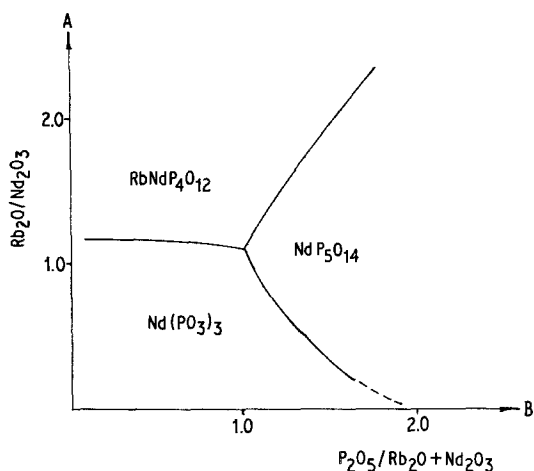


Figure 1 AB diagram showing fields of crystallization of different phases in the system $\text{Rb}_2\text{O}-\text{Nd}_2\text{O}_3-\text{P}_2\text{O}_5-\text{H}_2\text{O}$.

cations in aqueous solutions exist as nezoite complexes [11]. Depending upon the growth conditions these complexes interact among themselves to form neodymium nezoite networks in which phosphoro-oxygen tetrahedra form $[\text{PO}_3]^{-1}$ chains or $[\text{P}_4\text{O}_{12}]^{-4}$ rings. The phosphoro-oxygen anionic configuration determines the concentration of H_2O and hence, in turn depends upon its partial pressure. Since the equilibrium in phosphate systems establishes slowly, the greater is the probability of simultaneous existence of many types of phosphoro-oxygen anions [12]. Under these conditions the metastable phases crystallize easily. Due to the simultaneous nucleation and crystallization of many RbNd phosphates, the growth of large monocrystals of RbNd phosphates is difficult.

We studied the phase formation in the system $\text{Rb}_2\text{O}-\text{R}_2\text{O}_3-\text{P}_2\text{O}_5-\text{H}_2\text{O}$ (where $\text{R} = \text{La}$ to Lu) within the temperature range 300 to 800°C particularly, in the field of stability of mixed alkaline rare earth phosphates. The results of the experiments are shown in Fig. 2. As in the previous system, here also at $\leq 550^\circ\text{C}$ three crystal-

line phases $\text{RbR}[\text{P}_4\text{O}_{12}]-\text{C}$; $\text{RbR}[\text{P}_4\text{O}_{12}]-\text{A}$ and $\text{RbR}(\text{PO}_3)_4-\text{VI}$ crystallize simultaneously. The tetrametaphosphates are characteristic of RbR phosphates containing larger rare earth cations (La to Gd). In the system investigated there are two ring types and two chain types of phosphates. Both the tetrametaphosphates, $\text{RbR}[\text{P}_4\text{O}_{12}]-\text{C}$ and $\text{RbR}[\text{P}_4\text{O}_{12}]-\text{A}$, change over to tetrapolyphosphates at $\approx 550^\circ\text{C}$. The boundaries of the morphotropic transformations are fixed at Eu and Gd for $\text{RbR}[\text{P}_4\text{O}_{12}]-\text{C}$ and $\text{RbR}[\text{P}_4\text{O}_{12}]-\text{A}$, respectively. The next morphotropic transition is fixed at Er, when $\text{RbR}[\text{P}_4\text{O}_{12}]-\text{A}$ changes over to $\text{RbR}(\text{PO}_3)_4-\text{VI}$. Thus, for groups (La to Eu) there are four polymorphic modifications, for Gd there are three polymorphic modifications, for the Tb to Er group there are two polymorphic modifications and finally for the Tm to Lu group there is only one polymorphic modification (Fig. 2).

3. Crystal chemistry

Among the mixed rubidium rare earth phosphates there are four structure types: two chain types ($\text{TlNd}(\text{PO}_3)_4$ [13] and $\text{CsPr}(\text{PO}_3)_4$ [14] – tetrapolyphosphates) and two ring phosphates ($\text{CsNd}[\text{P}_4\text{O}_{12}]-\text{C}$ [15] and $\text{NH}_4\text{Pr}[\text{P}_4\text{O}_{12}]-\text{A}$ [16] – tetrametaphosphates). The difference between the two types of polyphosphates $\text{RbNd}(\text{PO}_3)_4-\text{IV}$ and $\text{RbNd}(\text{PO}_3)_4-\text{VI}$ lies in the cationic arrangement. In the structure of $\text{RbNd}(\text{PO}_3)_4-\text{IV}$ each rubidium atom is surrounded by nine oxygen atoms to form a nine-sided polyhedron. The rubidium polyhedra are arranged as isolated pairs connected to each other along the edges. The neodymium atoms are represented as isolated irregular eight-sided polyhedra, which are connected with four rubidium polyhedra to form a three-dimensional network and they form together eight-membered polyphosphate chains. Each neodymium polyhedron is surrounded by four rubidium polyhedra (two along the edges and two at the corners). Each neodymium polyhedron is surrounded by three

TABLE I X-ray data for $\text{RbNdP}_4\text{O}_{12}$

Phosphate	System	Space group	Cell parameters (nm)			Axial angle (degrees)	Contents of the unit cell, Z	Reference
			a	b	c			
$\text{RbNd}[\text{P}_4\text{O}_{12}]-\text{C}$	Cubic	$I\bar{4}3d$	1.512	—	—	—	12	Present work
$\text{RbNd}[\text{P}_4\text{O}_{12}]-\text{C}$	Monoclinic	$C2/c$	0.7845	1.2691	1.0688	112.34	4	[9]
$\text{RbNd}(\text{PO}_3)_4-\text{VI}$	Monoclinic	$P2_1$	0.7085	0.9041	0.8790	100.12	2	Present work
$\text{RbNd}(\text{PO}_3)_4-\text{VI}$	Monoclinic	$P2_1/b$	1.0473	1.2898	0.9042	126.00	4	[10]

† Indexing is done according to [8].

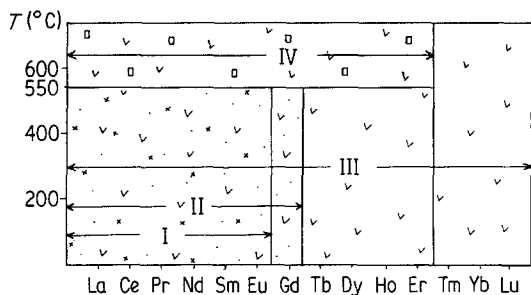


Figure 2 Distribution of different structure types of $\text{RbRP}_4\text{O}_{12}$.

polyphosphate chains by taking five terminal oxygen atoms from the first chain, two terminal oxygen atoms from the second and one terminal oxygen atom from the third chain ($5 + 2 + 1$). The other tetraphosphate $\text{RbNd}(\text{PO}_3)_4$ -VI is isostructural with $\text{CsPr}(\text{PO}_3)_4$ [14]. Here, both neodymium and rubidium atoms are represented as isolated polyhedra surrounded by eight oxygen atoms. Each neodymium polyhedron is connected with one rubidium polyhedron along an edge and two rubidium polyhedra at the corners. Similarly each neodymium polyhedron is connected with two polyphosphate chains by taking seven terminal oxygen atoms from the first and only one terminal oxygen atom from the second chain ($7 + 1$).

The structures of both modifications of tetrametaphosphates are close to one another. The difference between the two exists in the nature of filling of the cavities existing between the phosphoro-oxygen rings $[\text{P}_4\text{O}_{12}]$. In the structure of $\text{RbNd}[\text{P}_4\text{O}_{12}]$ -A these cavities are occupied alternatively by the atoms of rubidium and neodymium in the form of irregular eight-sided polyhedra. The rubidium and neodymium polyhedra are facially connected to each other forming isolated dimers of $[\text{RbNdO}_{10}]$. The other tetrametaphosphate $\text{RbNd}[\text{P}_4\text{O}_{12}]$ -C is isostructural with $\text{CsNd}[\text{P}_4\text{O}_{12}]$ -C, whose structure is represented as four-membered rings of $[\text{P}_4\text{O}_{12}]$ anions [15]. Here the cavities between the rings are occupied by two or three neodymium and two rubidium atoms which form isolated dimers of $[\text{RbNdO}_{10}]$.

The interatomic distances in RbNd phosphates are given in Table II. In polyphosphates the bridging P-O bond lies in the interval 0.1565 to 0.1622 nm (the average bond distance is 0.1601 nm) and the difference in the bond distances (ΔS) is 0.0086 nm. The interatomic distances of P-O terminal bonds lie in the interval

0.1422 to 0.1494 nm (average bond distance is 0.1477 nm) and the difference in the bond distances (ΔS) is 0.0047 nm.

In tetrametaphosphates the P-O distances of bridging bonds lie in the interval 0.1568 to 0.1611 nm (average bond distance is 0.1592 nm) and the difference in bond distances (ΔS) is 0.0033 nm. The bond distances of terminal bonds lie in the interval 0.1466 to 0.1491 nm (average bond distance is 0.1482 nm) and the difference in bond distances (ΔS) is 0.0016 nm. The average values of P-O bond distances are closer to the average values of terminal and bridging bonds characteristic for condensed phosphates (0.148 and 0.161 nm respectively). The sizes of the P-O polyhedra in polyphosphate chains vary slightly ($\Delta S = 0.0033$ and 0.0012 nm). The P-O tetrahedra in tetrametaphosphates have almost a constant size in the rings ($\Delta S = 0.0004$ and 0.0001 nm).

4. Infrared spectra

We have carried out a systematic characterization of rare earth phosphates in our laboratory using various methods like X-ray diffraction, infrared (IR) and laser spectroscopy, differential thermal analysis (DTA), ionic conductivity measurements etc. IR spectroscopy is one of the best available methods of understanding the minute structural details in $[\text{PO}_4]$ tetrahedra. In previous work we have reported on the IR spectroscopy of $\text{CsRP}_4\text{O}_{12}$ crystals [17]. In the present work we report on the IR spectroscopy of $\text{RbRP}_4\text{O}_{12}$ crystals, particularly $\text{RbNdP}_4\text{O}_{12}$ from each structural modification.

IR spectra of $\text{RbNdP}_4\text{O}_{12}$ crystals were registered in the range 1800 to 400 cm^{-1} using an IR spectrophotometer UR-low (GDR). It is well known that tetraphosphates exhibit diverse spectra consisting of five groups of absorption bands (Fig. 3). The results of IR spectroscopy well corroborate the X-ray analysis for $\text{RbNdP}_4\text{O}_{12}$. IR spectroscopy of $\text{RbNdP}_4\text{O}_{12}$ crystals divides them into two groups belonging to four structure types: $\text{RbNd}(\text{PO}_3)_4$ -IV; $\text{RbNd}(\text{PO}_3)_4$ -VI and $\text{RbNd}[\text{P}_4\text{O}_{12}]$ -C; $\text{RbNd}[\text{P}_4\text{O}_{12}]$ -A. The vibrational frequencies ($\nu \text{ cm}^{-1}$) of RbNd phosphates are given in Table III.

The spectrum of $\text{RbNd}[\text{P}_4\text{O}_{12}]$ -A has intensity bands in the range 1280 to 1200 cm^{-1} like the other cyclic phosphates, a series of other medium intensity bands in ranges 1140 to 1110 cm^{-1} and 595 to 470 cm^{-1} , and a number of weaker bands

TABLE II Bond distances in tetraphosphates in (nm)

	RbNd[P ₄ O ₁₂]-A [9]		RbNd(PO ₃) ₄ -IV [10]
P ₁ -O ₁	0.1599(8)	P ₁ -O ₁	0.1617
P ₁ -O ₂	0.1571(8)	P ₁ -O ₂	0.1599
P ₂ -O ₂	0.1605(8)	P ₂ -O ₂	0.1595
P ₂ -O ₃	0.1568(7)	P ₂ -O ₃	0.1593
P-O (min)	0.1568	P ₃ -O ₃	0.1616
P-O (max)	0.1605	P ₃ -O ₄	0.1605
P-O (average)	0.1586	P ₄ -O ₄	0.1605
ΔS (bridging bonds)	0.0037	P ₄ -O ₅	0.1581
P ₁ -O ₅	0.1466(7)	P-O (min)	0.1581
P ₁ -O ₆	0.1484(7)	P-O (max)	0.1617
P ₂ -O ₇	0.1488(8)	P-O (average)	0.1601
P ₂ -O ₈	0.1474(8)	ΔS (bridging bonds)	0.0036
P ₃ -O ₉	0.1466(7)	P ₁ -O ₆	0.1484
P ₃ -O ₁₀	0.1484(7)	P ₁ -O ₇	0.1484
P ₄ -O ₁₁	0.1488(8)	P ₂ -O ₈	0.1478
P ₄ -O ₁₂	0.1474(8)	P ₂ -O ₉	0.1489
P-O (min)	0.1466	P ₃ -O ₁₀	0.1476
P-O (max)	0.1488	P ₃ -O ₁₁	0.1485
P-O (average)	0.1478	P ₄ -O ₁₂	0.1464
ΔS (terminal bonds)	0.0022	P ₄ -O ₁₃	0.1481
P ₁ -O (average)	0.1534	P-O (min)	0.1464
P ₂ -O (average)	0.1530	P-O (max)	0.1489
P ₃ -O (average)	0.1534	P-O (average)	0.1480
P ₄ -O (average)	0.1530	ΔS (terminal bonds)	0.0025
ΔS (average)	0.0004	P ₁ -O (average)	0.1546
Coordination number		P ₂ -O (average)	0.1538
of Nd	8	P ₃ -O (average)	0.1545
Nd-O (min)	0.2406	P ₄ -O (average)	0.1532
Nd-O (max)	0.2450	P-O (average)	0.1542
Nd-O (average)	0.2426	ΔS (average)	0.0012
ΔS	0.0044	Coordination number	
Shortest Nd-Nd	0.6129	of Nd	8
Coordination number		Nd-O (min)	0.2366
of Rb	10	Nd-O (max)	0.2510
Rb-O (average)	0.3146	Nd-O (average)	0.2442
		ΔS	0.0144
		Shortest Nd-Nd	0.5756
		Coordination number	
		of rubidium	9
		Rb-O (average)	0.3206

(Fig. 3). The X-ray study confirms that this cyclic phosphate belongs to the monoclinic system. The spectrum of RbNd[P₄O₁₂]-A is very close to that of RbEu[P₄O₁₂] [18] and KNd[P₄O₁₂] [5]. This indicates that they are isostructural. The minute differences are due to the changes in the cationic arrangement.

The spectrum of RbNd[P₄O₁₂]-C has intensity bands at 1270, 1110 and 530 cm⁻¹. The spectrum varies widely from earlier ones. This is due to changes in the arrangement of [PO₄]³⁻ anions. The structure of this modification has not been studied so far by X-ray diffraction methods. The absorption spectrum of RbNd[P₄O₁₂]-C is very close to

that of CsNd[P₄O₁₂]-C, whose structure has been refined by X-ray diffraction methods [13].

The spectrum of RbNd(PO₃)₄-IV has intensity bands in the range 1310 to 1260 cm⁻¹, and a series of medium intensity bands in the range 1100 to 900 cm⁻¹. This spectrum is very close to that of CsNd(PO₃)₄-IV.

The spectrum of RbNd(PO₃)₄-VI has intensity bands in the range of 1300 to 1200 cm⁻¹ and a series of other medium and less intense bands in the ranges 1190 to 1110 and 540 to 450 cm⁻¹. The spectrum of this compound has a highly complex and fine structure, particularly in the range 1200 to 1100 cm⁻¹.

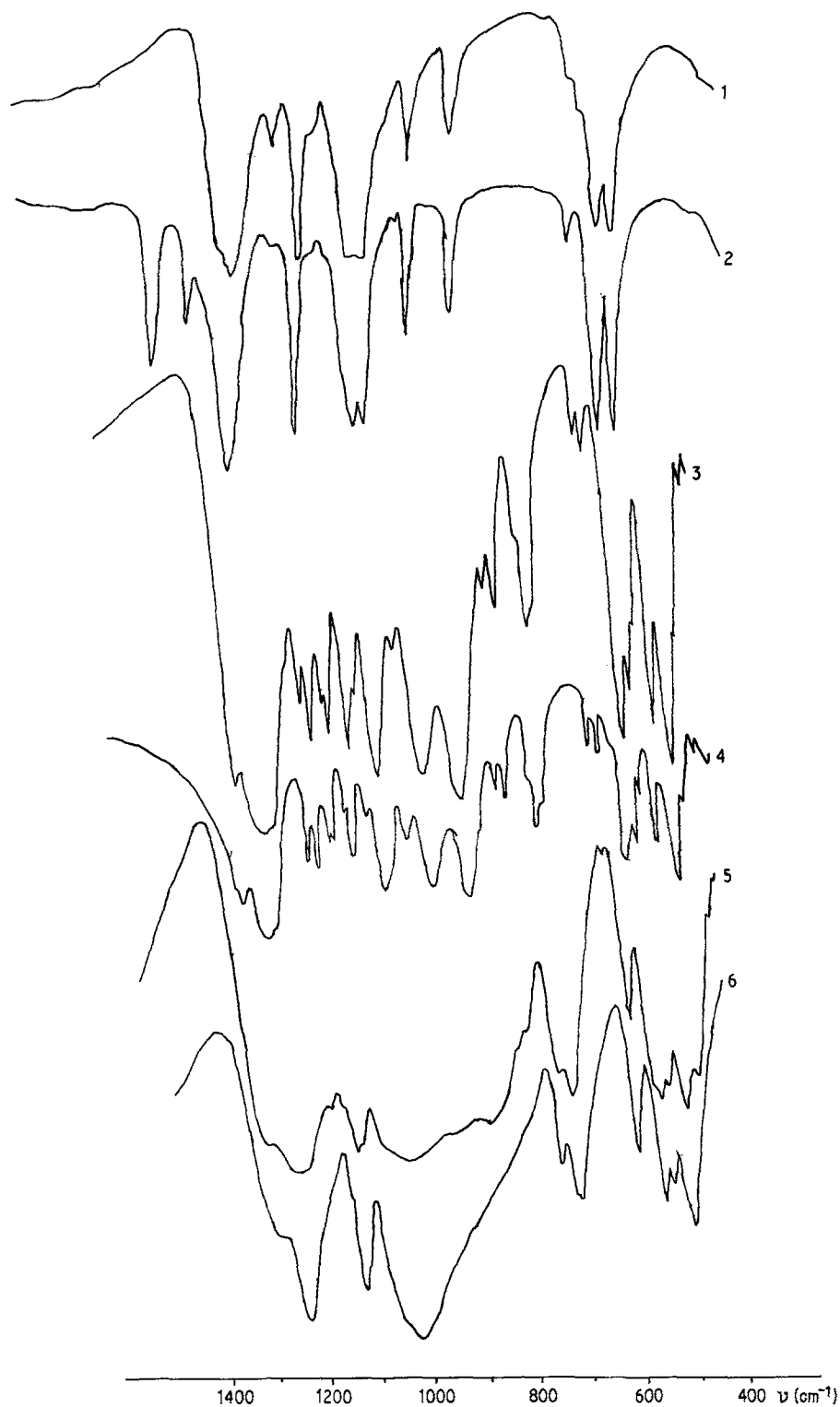


Figure 3 IR spectra of mixed alkaline rare earth phosphates: (1) $\text{RbNd}[\text{P}_4\text{O}_{12}]\text{-C}$; (2) $\text{CsNd}[\text{P}_4\text{O}_{12}]\text{-C}$; (3) $\text{RbNd}(\text{PO}_3)_4$ IV; (4) $\text{CsNd}(\text{PO}_3)_4\text{-IV}$; (5) $\text{RbNd}(\text{PO}_3)_4\text{-VI}$; and (6) $\text{RbNd}[\text{P}_4\text{O}_{12}]\text{-A}$.

TABLE III Vibrational frequencies (ν cm⁻¹) of RbNd phosphates

Vibration	Chain type		Ring type	
	RbNd(PO ₃) ₄ -VI	RbNd(PO ₃) ₄ -IV	RbNd[P ₄ O ₁₂]-C	RbNd[P ₄ O ₁₂]-A
ν_{as} OPO	1300- <u>1230</u> -1200	1290- <u>1240</u> -1200	1290- <u>1260</u> -1230	1260- <u>1230</u> -1200
ν_s OPO	1140-1100	1170- <u>1145</u> -1100	1160- <u>1105</u> -1075	1140-1110
ν_{as} POP	1065- <u>1030</u> -1010	-1020-	995- <u>950</u> -940	1060- <u>1020</u> -970
ν_s POP	720-690-450	805-700	850-700	740-660
δ OPO	605- <u>480</u> -450	605- <u>450</u> -435	575- <u>525</u> -500	600- <u>490</u> -465
δ POP	< 400	< 400	< 400	< 400

Underlined values represent intensive peaks in the spectra.

With an increase in the degree of condensation of the anionic group, there occurs an increase in the number of absorption bands of phosphoro-oxygen anions in the spectra. Thus, in orthophosphates only two absorption bands are seen, whereas five to six absorption bands are seen in ultra- and polyphosphates: ν_{as} OPO, ν_s OPO, ν_{as} POP, ν_s POP, δ OPO and δ POP [17]. The interaction of the P-O bands with one another splits each valence vibration into two components, namely, ν_s OPO, ν_{as} OPO, ν_s POP and ν_{as} POP. It is clearly seen from the spectra of RbNdP₄O₁₂, that the higher the OPO angle, the greater will be the splitting between the two components of the frequency band. The cyclic phosphates have less splitting in the valence vibration ν_{as} OPO and ν_s OPO ($\Delta\nu \approx 150$ cm⁻¹) than the chain phosphates ($\Delta\nu \approx 200$ cm⁻¹).

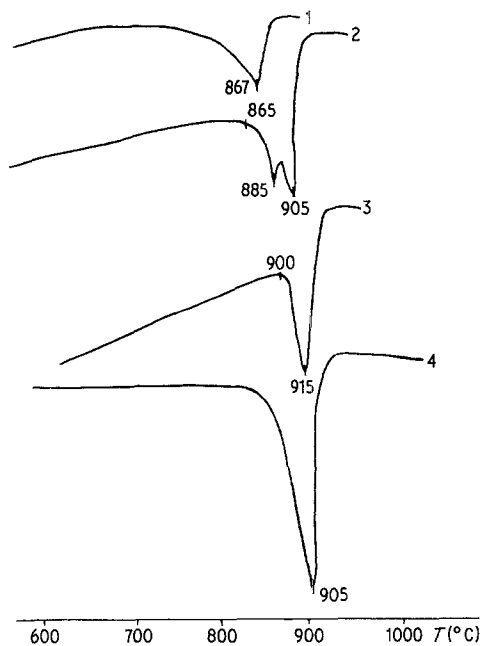


Figure 4 DTA curves for RbNd phosphates. (1) RbNd[P₄O₁₂]-C; (2) RbNd(PO₃)₄-VI; (3) RbNd[P₄O₁₂]-A; and (4) RbNd(PO₃)₄-IV.

5. DTA and laser properties

The differential thermal analysis of all the four modifications of RbNd phosphates shows that RbNd phosphates melt incongruently at the following temperatures:

RbNd[P ₄ O ₁₂]-A	915° C
RbNd[P ₄ O ₁₂]-C	867° C
RbNd(PO ₃) ₄ -VI	905° C
RbNd(PO ₃) ₄ -IV	905° C

The results of the DTA are shown in Fig. 4. It is observed that RbNd[P₄O₁₂]-A initially changes over to RbNd(PO₃)₄-IV at 885° C and finally melts at 905° C.

The basic laser characteristics of RbNdP₄O₁₂ crystals are given in Table IV. We obtained RbNd phosphates with optically inactive rare earth ions such as La³⁺, Ce³⁺ and Gd³⁺ replacing Nd³⁺ ions up to 1.0%. It is interesting to note that the RbNd[P₄O₁₂]-C crystals (100% neodymium concentration) obtained at lower temperatures (~350° C) have the highest value of fluorescent lifetime ($\tau = 150 \pm 10$ μ sec) in comparison with other rare earth phosphates containing 100% of the active ions in their composition. Therefore, RbNdP₄O₁₂ crystals are potentially good miniature laser materials.

Conclusions

1. Investigations of the system Rb₂O-R₂O₃-P₂O₅-H₂O within the temperature range 300 to 800° C show that there are four structural modifications among RbRP₄O₁₂.

2. Under the same physico-chemical conditions different polymorphic modifications of RbRP₄O₁₂ crystallize.

3. The X-ray and infrared studies show that there are two chain types and two ring types of phosphates in the system investigated.

TABLE IV Laser properties of RbNd phosphates

Phosphate	λ_{rad} (μm)	Number of atoms, $N (\times 10^{21})$	Shortest Nd-Nd distance	Lifetime ($\pm 10 \mu\text{sec}$)		Quantum output, η
				τ	τ_0	
RbNd[P ₄ O ₁₂]-C	1051	3.47	unknown	150	360	0.41
RbNd[P ₄ O ₁₂]-A	1050	4.09	0.6129	100	290	0.34
RbNd(PO ₃) ₄ -IV	1052	4.01	0.6130	90	280	0.32
RbNd(PO ₃) ₄ -VI	1050	3.27	0.7260	110	350	0.31

4. Only the larger rare earths (La to Gd) form ring structures among the tetraphosphates.

5. The crystal chemistry of RbRP₄O₁₂ shows that [PO₄] tetrahedra in the cyclophosphates are less disturbed (less irregular) than in the chain phosphates.

6. The study of the laser characteristics of RbNdP₄O₁₂ shows that RbNdP₄O₁₂ crystals are potentially good miniature laser materials.

References

1. B. N. LITVIN and K. BYRAPPA, *J. Cryst. Growth* **51** (1981) 470.
2. K. BYRAPPA and G. I. DOROKHOVA, *J. Mater. Sci.* **16** (1981) 3244.
3. J. NAKANO, T. YAMADA and S. MIYAZAWA, *J. Amer. Ceram. Soc.* **62** (1979) 466.
4. J. NAKANO, S. MIYAZAWA and T. YAMADA, *Mater. Res. Bull.* **14** (1979) 21.
5. B. N. LITVIN, O. S. TARASENKOVA, V. A. MASLOBOEV, N. V. VINOGRADOVA and N. N. CHUDINOVA, *Izvestia Academy Nauk USSR, Inorg. Mater.* **18** (1982) 298.
6. B. N. LITVIN, K. BYRAPPA, V. A. MASLOBOEV, N. N. CHUDINOVA and N. V. VINOGRADOVA, *ibid.* **17** (1981) 1438.
7. B. N. LITVIN, K. BYRAPPA and L. G. BEBIKH, *Prog. Cryst. Growth Charact.* **3** (1981) 257.
8. K. K. PALKINA, N. N. CHUDINOVA, B. N. LITVIN and N. V. VINOGRADOVA, *Izvestia Academy Nauk USSR, Inorg. Mater.* **17** (1981) 1501.
9. H. KOIZUMI and J. NAKANO, *Acta Crystallogr.* **B33** (1977) 2680.
10. K. BYRAPPA, O. S. PHILEPENKO and B. N. LITVIN, *Probl. Crystallogr.* **3** (1981) 264.
11. B. N. LITVIN, *Probl. Crystallogr.* **3** (1981) 93.
12. J. R. VAN WAZER, "Phosphorus and Its Compounds" Vol. 1, (Interscience, New York, 1958) Chap. IV.
13. K. K. PALKINA, V. Z. SAIFUDDINOV, V. G. KUZNESTOV and N. N. CHUDINOVA, *Doklady Academy Nauk USSR* **237** (1977) 837.
14. K. K. PALKINA, S. I. MAKSIMOVA and V. G. KUZNESTOV, *Izvestia Academy Nauk USSR, Inorg. Mater.* **14** (1978) 284.
15. K. K. PALKINA, S. I. MAKSIMOVA and N. T. CHIBISKOVA, *Doklady Academy Nauk USSR* **257** (1981) 357.
16. R. MASSE, J. C. GUITTEL and A. DURIF, *Acta Crystallogr.* **33** (1977) 630.
17. K. BYRAPPA, I. I. PLYUSNINA and G. I. DOROKHOVA, *J. Mater. Sci.* **17** (1982) 1847.
18. V. A. MADII, Yu. I. KRASILOV, V. A. KIZEL, Yu. V. DENISOV, N. N. CHUDINOVA and N. V. VINOGRADOVA, *Izvestia Academy Nauk USSR, Inorg. Mater.* **14** (1978) 2061.
19. W. BUES and H. W. GEHRKE, *Zeit. für Anorg. Chem.* **Bd 288** (1956).

Received 26 October

and accepted 29 November 1982